Continuous Strain Measurements During and Preceding Episodic Creep on the San Andreas Fault

M. J. S. JOHNSTON, A. C. JONES, AND W. DAUL

Office of Earthquake Studies, U.S. Geological Survey, Menlo Park, California 94025

Continuous strain measurements from 3 three-component invar wire strainmeters installed 1200, 1500, and 1700 m from the San Andreas fault indicate no observable strain change at the instrument resolution ($<10^{-8}$) during 10 episodic creep events on the fault. These strain observations indicate that the slip area responsible for the creep observations is near surface and of quite limited extent. The episodic creep character probably results from the failure properties of near-surface materials rather than general fault behavior, which is better indicated perhaps by averaged creep. Deeper slower slip apparently loads the surface material. Longer-term strain changes ($\sim 10^{-7}$) do occur, but the form of the signal is not what would be expected from simple models, nor is it consistent, for successive events. The amplitude does not increase with creep event amplitude, and similar changes occur without creep events. Deeper slip on the San Andreas fault apparently is smoother than would be inferred from the duration of episodic creep observations. Unfortunately, signal discrimination capability gets worse at longer periods and needs improvements if slow deformation waves are to be detected at strain levels below 10^{-7}.

INTRODUCTION

Aseismic fault slip or fault creep accounts for almost all horizontal displacement on the San Andreas fault in central California [*Savage and Burford*, 1973; *Wesson et al.*, 1973]. The mechanics of this type of fault failure and its relation to earthquake-generating failure are poorly understood. *Savage* [1971] and *Ida* [1974] have proposed models of slow propagating fault slip as a mechanism for loading to failure successive sections of active faults. Continuous measurements of the strain and tilt fields along the San Andreas fault where aseismic fault slip occurs provide an opportunity to quantify the mechanism of active fault slip.

The primary features of the present fault creep observations are the episodic character in some locations (creep events) and the smooth or continuous character in others [*Nason et al.*, 1974; *Yamashita and Burford*, 1973]. There may be indications of propagation of a deformation wave along the fault in the pattern of creep onset times at various points along the fault. The events have slip amplitudes of a few millimeters and occur within a day or so at different locations over at least a few kilometers [*C. Y. King et al.*, 1973].

The occurrence of a number of creep events near three-component strainmeters at two different locations along the San Andreas affords an opportunity to search for the transient strains that must be associated with each creep event. The model of creep events proposed by *Frank* [1973] would predict transient strains at about 1 km from the fault of more than 10^{-7}.

A strain step on a single-component strainmeter together with changes in tilt and water well level has been associated with a creep event sequence by *Mortensen et al.* [1977]. Other transient strains for which there are no actual observations of fault displacement have been reported by *Bufe and Tocher* [1974] and *G. C. P. King et al.* [1975]. Transient tilts just preceding and coincident with three creep events seen on an array of creepmeters have been reported by *Johnston et al.* [1976] and discussed in detail by *McHugh and Johnston* [1976]. These and other creep-related tilt events have been clearly identified only on instruments less than 0.5 km from the fault. The peak-to-peak tilt amplitudes were less than 5×10^{-7} rad at about 0.4 km from the fault for a 4-mm creep event on the fault. At a distance of 1.2 km the creep-related tilt was apparently below the instrument resolution (10^{-8} rad).

In this paper we summarize the continuous strain data obtained at two particular locations near the San Andreas fault where frequent episodic creep events occur and discuss the implications of these data for fault creep models. At these locations, at least one three-component strainmeter is installed at a distance of about 1 to 1.7 km from the fault. A total of 10 creep events have occurred on the fault since early 1974. Five of these had slip amplitudes of more than 1 mm, the largest being about 5 mm.

INSTRUMENTATION

The strainmeters are installed 1200–1700 m from the section of the fault where the creep events occur. The instrument locations with respect to the fault and creepmeters are shown in Figure 1. The strainmeters have an invar wire reference similar to that used by *G. C. P. King and R. G. Bilham* [1976] and others, with end mounts anchored to the top of aged steel pipe grouted with expanding grout (Chemcomp by Kaiser Cement Company) into a shallow 4.5-m-deep borehole as indicated in Figure 2. The wire between anchor points is 10 m long and is encased in polyvinyl chloride pipe in a shallow 1.5-m-deep trench. Relative strain is detected with a differential capacitance transducer [*Stacey et al.*, 1969] by transforming horizontal displacements to vertical displacements with a simple mechanical lever. The lever is made of stress-relieved stainless steel and is hinged with a stainless steel Cardon hinge, as shown in Figure 2. Stability of the displacement transducer was less than 10^{-8} m/month. This was measured by using fixed plates separated by quartz spacers. Linearity was less than 0.2% over the middle 80% of the range [*Gladwin and Wolfe*, 1975]. The strainmeter was calibrated by adding, with a precision micrometer, 10-μm displacements to the wire in order to obtain the scale factor conversion for the displacement transducer.

Earth tides are observed on these strainmeters. Records for the week October 1–8, 1975, which covers the time of a creep event on October 1 to be discussed later, are plotted together with theoretical earth strain tides in Figure 3. Some diurnal thermoelastic contamination is evident. This tends to interfere with various tidal frequencies.

Paper number 7B0805.

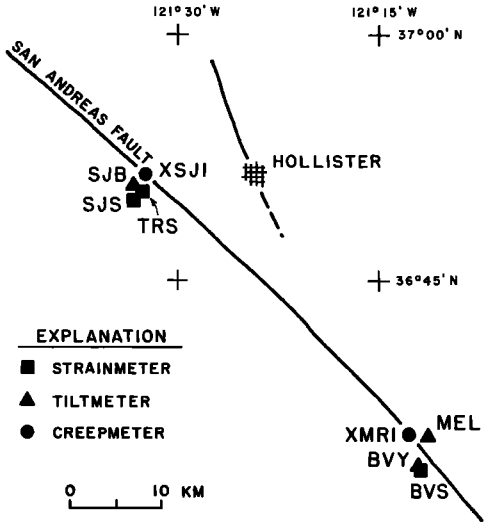

Fig. 1. Location of strainmeters SJS, TRS, BVS, and BV1S with respect to creepmeters XSJ1 and XMR1 on the San Andreas fault. Shown also are nearby tiltmeters SJB, NUT, BVL, and MEL. SJS, TRS, and BVS each consist of three components designated 1, 2, and 3. The components are orientated at 120° intervals in a strain rosette configuration. BVS1, TRS1, and SJS1 are all perpendicular to the fault. BVS2, TRS2, and SJS2 are in a clockwise sense from BVS1, etc., as shown; for example, in Figure 2, BV1S is parallel to BVS2.

DATA

From October 1, 1974, until May 30, 1976, four creep events have been recorded on the San Juan Bautista creepmeter and six events on the creepmeters at Melendy Ranch on the fault near the Bear Valley strainmeter. The records from these creepmeters at the time of the creep events, together with strainmeter records covering the same period, have been digitized and plotted on common time and amplitude scales. The location, occurrence time, amplitude, and approximate duration of each creep event is listed in Table 1 together with the nearest strainmeter(s) and the distance between the strainmeter(s) and the fault. Note that the creep amplitudes are measured on creepmeters oriented generally at 30° to the fault. Actual fault displacements will be a factor of 1.2 greater.

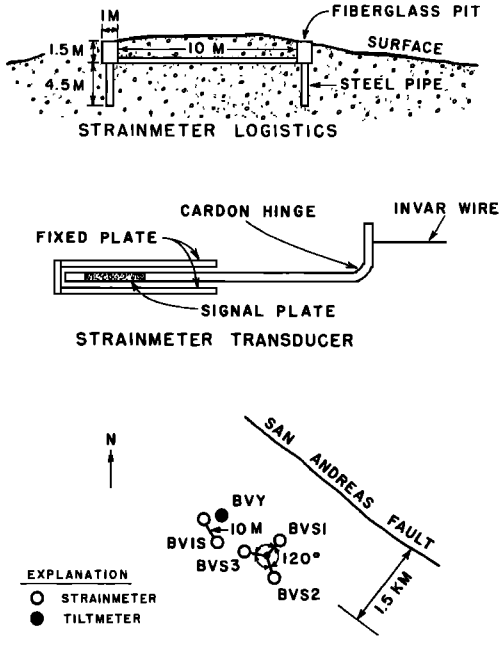

Fig. 2. Schematic representation of typical strainmeter installation and layout for BVS1, BVS2, BVS3, and BV1S.

Figure 4 shows the instrument locations and 12 hours of parallel strain and creep records for the three largest creep events at Bear Valley. The first occurred on October 3, 1974, with an amplitude of 2.28 mm. A single-component prototype strainmeter, BV1S was the only strainmeter in operation during this creep event. This meter is oriented approximately 30° to the fault and is 1.5 km from it. There is no apparent signal on the strain record during this 12-hour period, and certainly not with the form and amplitude ($\sim 10^{-7}$) expected for this strainmeter, as will be discussed later, on the basis of *Frank*'s [1973] model. Tilt records from the tiltmeters MEL and BVL during this creep event have been published by *Johnston et al.* [1976]. Tilts of a few parts in 10^7 were observed at MEL just prior to and during the creep event, but no tilt greater than 10^{-8} rad was observed at BVL.

The second creep event occurred on October 27, 1975. It had an amplitude of 2.4 mm. By this time a second strainmeter was installed and operating. Its components, BVS1, BVS2, and BVS3, were oriented 120° apart, as shown in Figure 2. This strainmeter was also 1.5 km from the fault, with BVS2 parallel to BV1S but separated from it by 0.4 km. Two small quakes were observed, one just before and one during the event. The third creep event occurred on January 25, 1976, with an amplitude of 1.71 mm. The only observable changes in the strainmeter records are caused by earth tides and diurnal thermoelastic contamination.

Figure 5 shows the strain and creep records for three similar but smaller creep events at the same site on September 24 and 27 and October 26, 1975. These events had amplitudes of 0.21, 0.17, and 0.11 mm, respectively.

Creep events at San Juan Bautista are generally of longer duration than those at Bear Valley. Figure 6 shows strainmeter and creepmeter records of four events at San Juan Bautista. The first creep event shown was on October 1, 1975. The amplitude was 2.4 mm, and it lasted about 18 hours. Thirty-six hours of parallel records from the creepmeter and from two of the three components of the San Juan strainmeter are shown. A small creep event, on September 30, preceded this one by a day. This event had an amplitude of 0.24 mm and is shown in the right-hand column of Figure 6. Twelve hours of data are

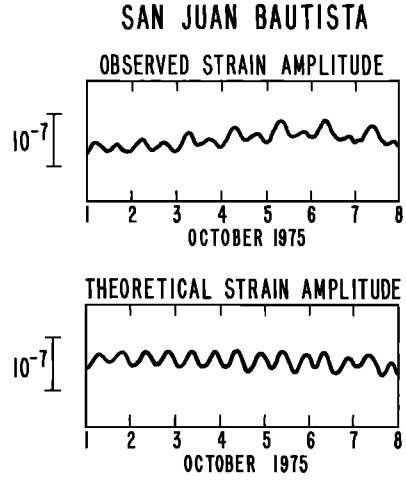

Fig. 3. Example of observed and theoretical earth strain tides recorded on SJS1 from October 1 to 8, 1975. A 2.4-mm creep event, to be discussed later, occurred on October 1, 1975.

TABLE 1. Location, Occurrence Time, Amplitude, and Duration of Creep Events

	Date	Start Time, UT	Amplitude, mm	Approximate Duration, hours	Nearest Strain Components With Data	Fault to Strainmeter Distance, km
			Creepmeter XMR1 (36°35.7'N, 121°11.2'W)			
1	Oct. 3, 1974	0837	2.28	2.5	BV1S	1.48
2	Sept. 24, 1975	0734	0.21	3.5	BV1S	1.48
					BVS1, BVS2, BVS3	1.5
3	Sept. 27, 1975	1319	0.17	3.0	BV1S	1.48
					BVS1, BVS2, BVS3	1.5
4	Oct. 26, 1975	2219	0.11	3.7	BV1S	1.48
					BVS1, BVS2, BVS3	1.5
5	Oct. 27, 1975	1830	2.41	2.0	BV1S	1.48
					BVS1, BVS2, BVS3	1.5
6	Jan. 25, 1976	1256	1.71	1.5	BV1S	1.48
					BVS1, BVS2, BVS3	1.5
			Creepmeter XSJ2 (36°50.2'N, 121°31.2'W)			
7	May 25, 1975	0516	4.03	96	SJS1, SJS2, SJS3	1.7
8	Sept. 30, 1975	1827	0.24	4	SJS1, SJS2, SJS3	1.7
9	Oct. 1, 1975	1034	2.40	18	SJS1, SJS2, SJS3	1.7
10	May 15, 1976	0243	4.85	105	SJS1, SJS2, SJS3	1.7
					TRS1, TRS2, TRS3	1.2

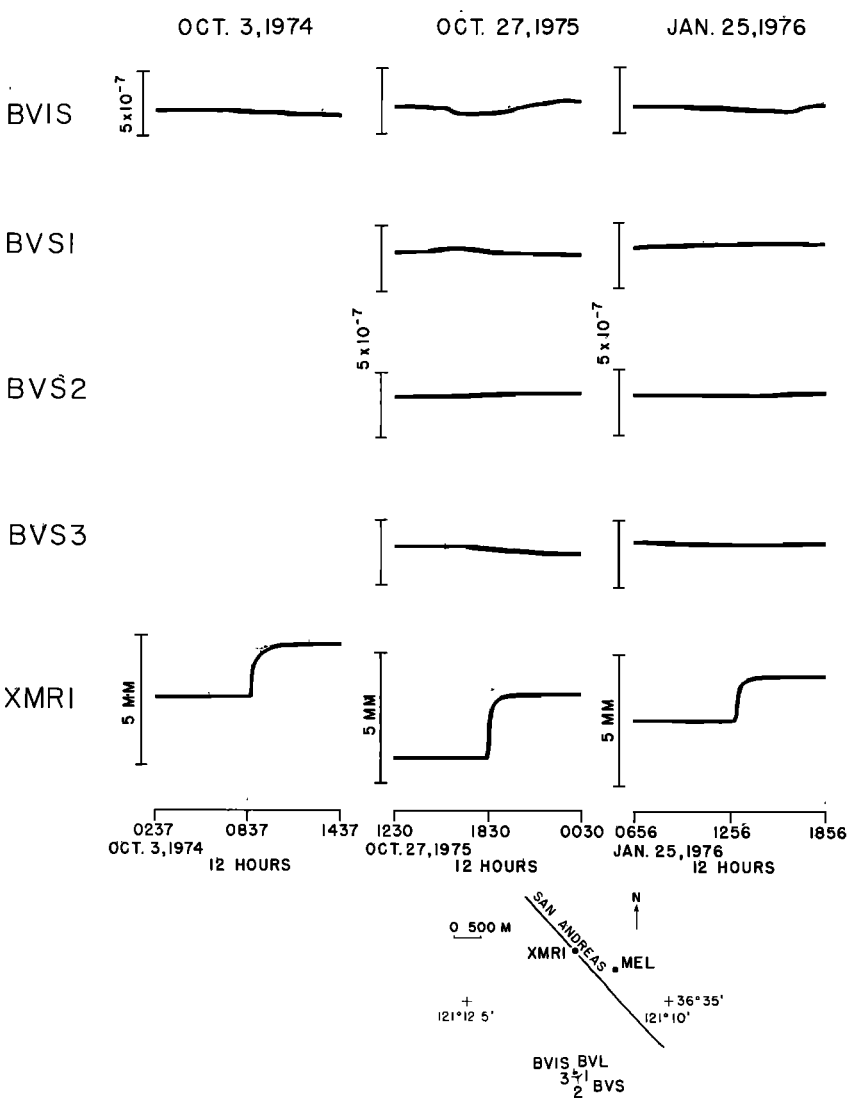

Fig. 4. Plots of 12 hours of parallel strain and creep data during the three largest creep events observed on XMR1. The relative instrument locations are shown also. Detailed creep onset times and amplitudes are listed in Table 1.

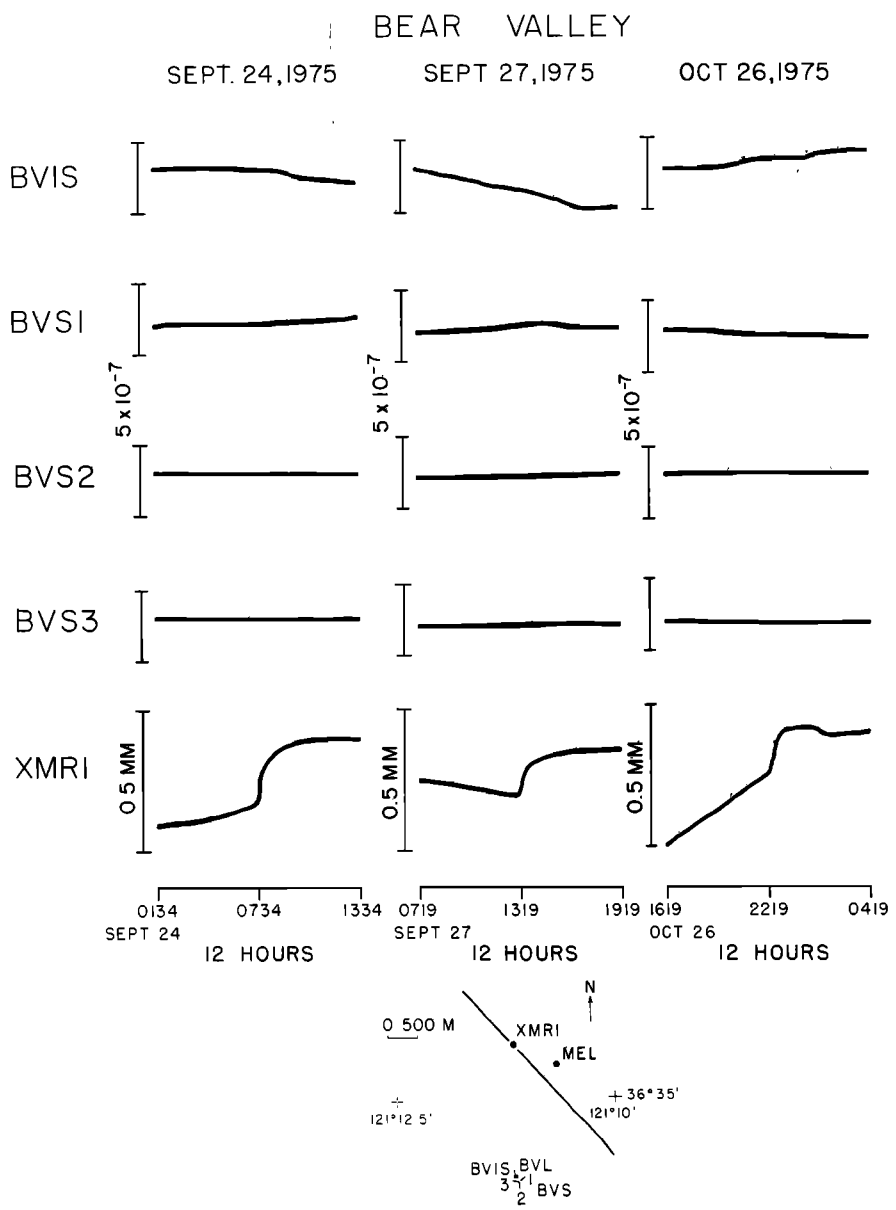

Fig. 5. Plots of 12 hours of parallel strain and creep data for the remaining three creep events listed in Table 1, for XMR1.

plotted for this event. The changes in amplitude in the strain records for both of these events were caused by earth tides. A third creep event on May 27, 1975, took place over a period of about 4 days and had an amplitude of 4.03 mm.

The final creep event (May 16, 1976) was another of 4–5 days duration. It had an amplitude of 4.85 mm. A second three-component strainmeter, TRS, was in operation in time for this creep event. For this event, possible creep-related changes in strain may be evident on SJS1 and TRS1.

It is possible, particularly for the events of short duration, that the surface creep events are triggered by deeper slower slip on the fault. To search for an indication of this, longer-term strain records were plotted that overlap by 20 days either way the occurrence time of the creep events. Figure 7 shows plots of 40 days of data from the Bear Valley strainmeter, that cover the times of the six creep events there. The creep event occurrence times are shown by arrows. Dilatant strains due to rainfall are also evident on these records when more than 4 cm of rain fell between February 4 and 10, 1976, at Bear Valley. The occurrence time and amount of rainfall are indicated by the solid bars.

A similar plot for the strain and creep data at San Juan Bautista is shown in Figure 8. The two largest creep events have durations of about 4 days, as is shown by the parallel bars above the arrow indicating the onset of creep. Rainfall is again shown as solid bars. The only significant rain was 1.1 cm on October 10, 1975.

DISCUSSION

Before attempting to argue whether any particular strain change is associated with a creep event or not, it is worthwhile to identify the form and amplitude of strain changes at these instrument sites on the basis of the models of fault slip. Perhaps the simplest such model is that by *Frank* [1973], who modeled the creep events as infinitely long edge dislocations in a homogeneous semi-infinite half space. When

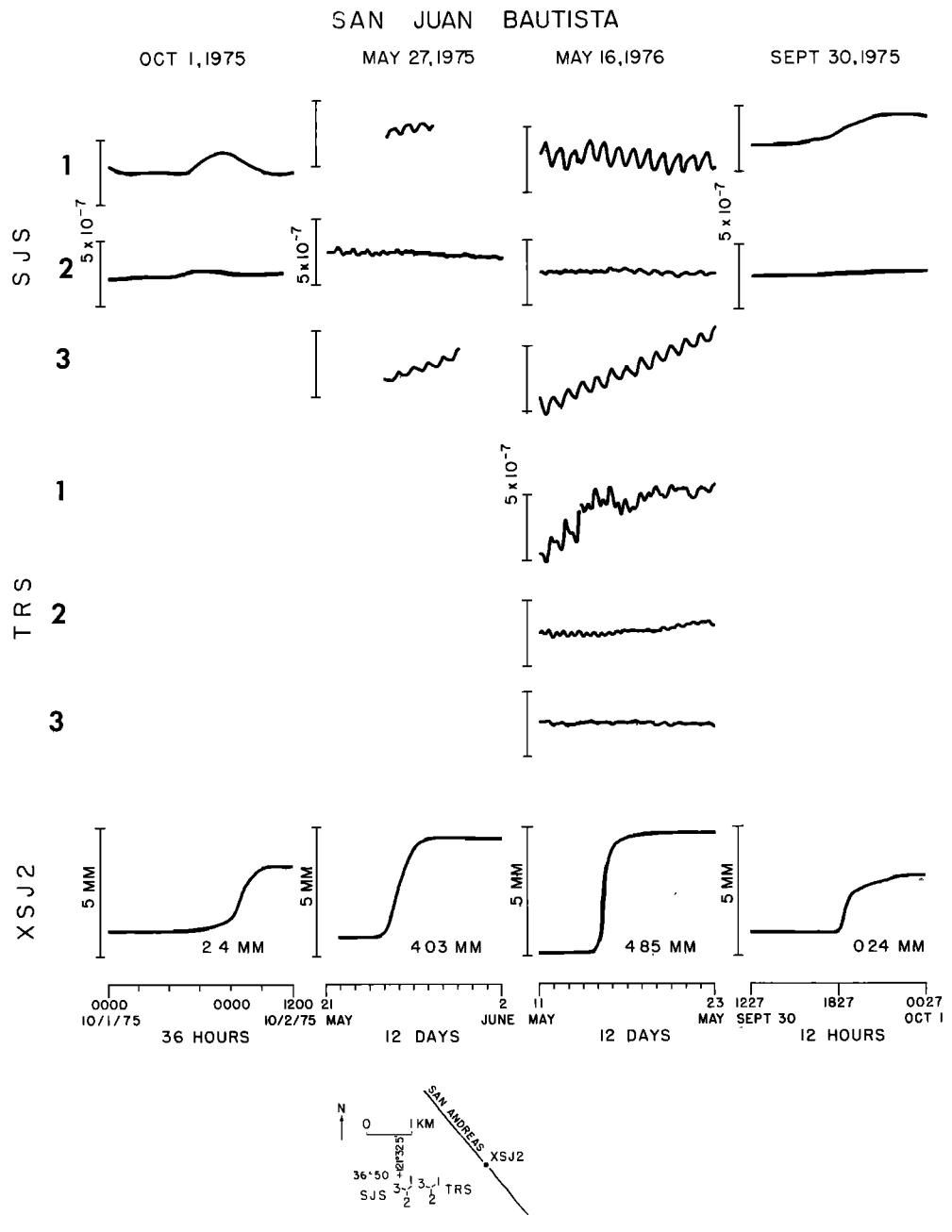

Fig. 6. Creep and strain-time history plots for the four creep events listed in Table 1 for XSJ2. Note that the time scales for these plots are 36 hours, 12 days, 12 days, and 12 hours.

this model is used, the microstrains for components at y kilometers from the fault and oriented N37°E, S23°E, and N83°W, such as at Bear Valley and San Juan Bautista, owing to a dislocation of slip amplitude of b millimeters at a point x kilometers along the fault, are given by

$$\epsilon_1 = -\frac{b}{4\pi y}\left\{\frac{(1-2\nu)}{(1+X^2)} - (1+2\nu)\left[\frac{2.0X^2}{(1+X^2)^2}\right]\right\} \quad (1)$$

$$\epsilon_2 = -\frac{b}{4\pi y}\left\{\frac{(1-2\nu)}{(1+X^2)} + (1+2\nu)\left[\frac{X^2}{(1+X^2)^2} + \frac{0.86X(1-X^2)}{(1+X^2)^2}\right]\right\} \quad (2)$$

$$\epsilon_3 = -\frac{b}{4\pi y}\left\{\frac{(1-2\nu)}{(1+X^2)} + (1+2\nu)\left[\frac{0.86X(1-X^2)}{(1+X^2)^2} - \frac{X^2}{(1+X^2)^2}\right]\right\} \quad (3)$$

where $X = x/y$ and ν is Poisson's ratio. The fault is oriented N53°W.

For slip velocities that are small in comparison with the shear or Rayleigh wave velocity this model can be used to approximate the dynamic strain-time history by introducing time into the position coordinates; e.g., $x = x_0 - ut$, where u is the velocity along the fault [*G. C. P. King et al.*, 1975].

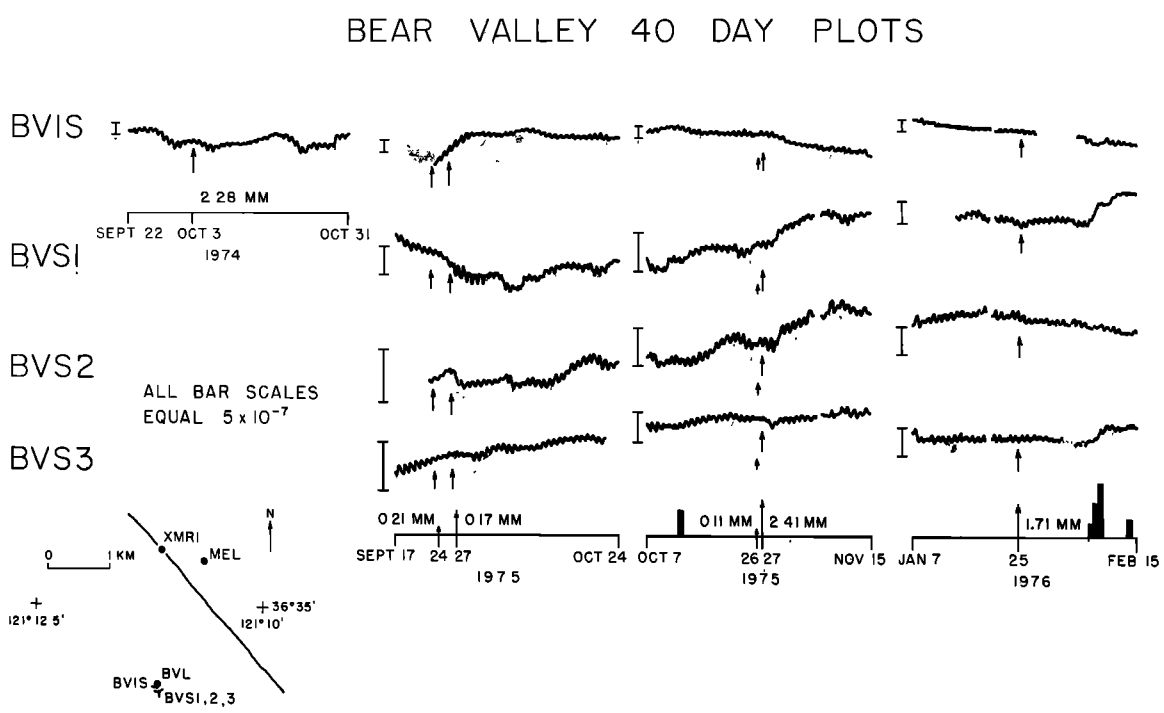

Fig. 7. Data from the Bear Valley strainmeters for 40 days spanning the occurrence time of creep events (marked with arrows) observed on XMR1. Rainfall is shown with solid bars. The largest amount is 1.8 cm on February 10.

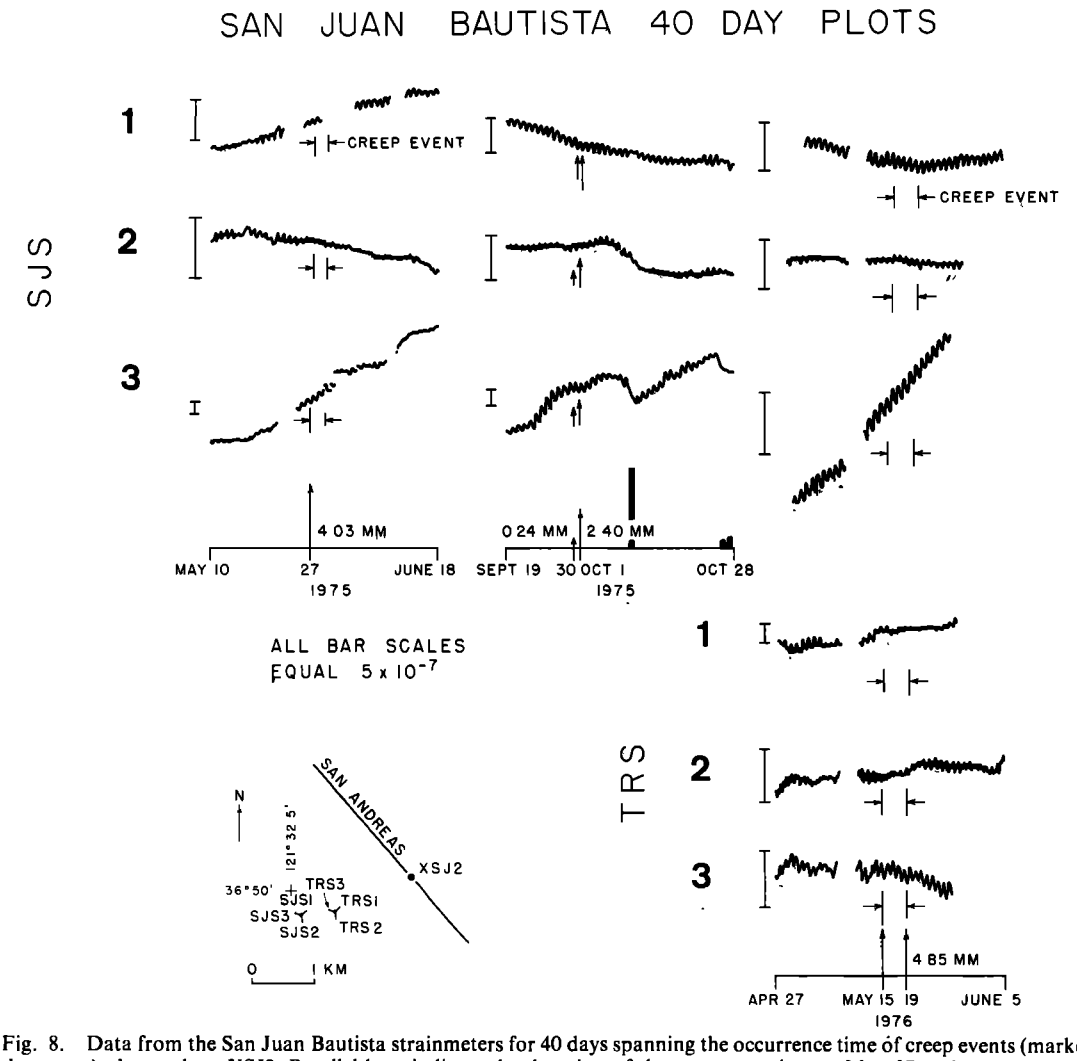

Fig. 8. Data from the San Juan Bautista strainmeters for 40 days spanning the occurrence time of creep events (marked with arrows) observed on XSJ2. Parallel bars indicate the duration of the events starting on May 27 and May 15, 1976. Rainfall is shown with solid bars. The largest amount is 2.4 cm on October 8.

If we take representative values of b, y, u, and ν to be 5 mm, 1.2 km, 1 km/h, and 0.25, respectively, the form of the strain-time history expected on the strainmeters is shown in Figure 9. These records are time compressed if u is increased and attenuated if y is increased.

It is immediately obvious that the observed strains at the time of the creep events do not have the form or the amplitude of these predicted strains. It is possible that the strains at these locations are of smaller amplitude, owing to a substantially decreased shear modulus in the fault zone. The results of *McHugh and Johnston* [1977] indicate that the concentration of strain fields near the fault due to about a factor of 4 decrease in fault zone rigidity could result in attenuated strain changes at the measurement points by up to a factor of 8. If this is the case it is possible that the strains expected from *Frank*'s [1973] model would not be clearly distinguishable in these data. However, a preliminary analysis of earth tides in data from these instruments with the techniques used by *Beaumont and Berger* [1974] indicates that no significant anomaly in average rigidity is apparent in this region.

Press [1965] modeled a finite dimension failure plane with a vertical rectangular dislocation loop and derived expressions for the strains on the free surface of an elastic half space. This solution was extended [*McHugh*, 1976] to model an expanding slip region and generalized to incorporate (1) variable geometry of the slip region, (2) slip-time functions that may be linear, quadratic, or exponential, (3) viscoelasticity, and (4) a slip distribution that may be uniform or nonuniform across the region. The model has been programed for a CDC 7600 computer by *McHugh* [1976] to calculate surface tilts and extended by *Mortensen et al.* [1977] to estimate strains at any point at the free surface. This model has been used to attempt a data fit.

Rigorous inversion is not possible with so few data. It is, however, instructive to determine the simplest models that are consistent with the data. Several general observations concerning the data can be best demonstrated with the aid of models. Classes of models have been run which have a slip distribution and maximum slip amplitude which are similar to those of the surface creep observations and in which all other parameters are systematically varied. The form of strain dependence on time at any point is, as might be expected, most critically dependent on the geometry of the slip region and its location with respect to the observation point. As an example, Figure 10 shows a range of strains expected at BVS1, BVS2, and BVS3 for a 3.0-mm slip event as a function of slip dimensions and position. The fault is in a half space of uniform shear modulus and starts to fail at a point $x_1 = 0$ over a depth of D kilometers. The slip propagates to the northwest along the fault, and, at any arbitrary point, once it is initiated it increases exponentially to its maximum value. The propagation velocity is arbitrarily set at 1 km/h. Lower or higher propagation velocities only expand or compress the time scale of the strain record. The form is unchanged.

It is evident that when the fault length and, to a lesser degree, the depth become comparable with or exceed the distance from strainmeter to fault, the maximum strains on the various components exceed 10^{-7}. For any moderate size slip region these strains should have been observed easily with the strainmeters.

A second point is that comparable signals are usually observed on all three strain components. Models, of course, can be built for which the strain on one component has a peak-to-peak value of less than 5×10^{-8}. However, it is quite difficult to minimize the strain to this level on two components simultaneously, and no geometry has yet been found that minimizes all three. In any case it would seem unlikely that any such particular model would apply in different locations and for many different events.

It would seem from these models that the size of the slipping region is less than 1 km in extent. The assumption most likely to be violated is that of a uniform shear modulus. If a shear modulus contrast of up to a factor of 4 is allowed and the strains are decreased by about an order of magnitude, some indications of consistent form in the strain records should still be evident by comparing records for different events. This appears not to be so, although signal stacking and other filtering techniques have not been tried.

The argument for consistency in the signals is important also when one is considering whether some of the changes in Figures 4, 5, and 6 that were previously attributed to tides or thermoelastic effects are in fact creep related.

If the region of failure giving rise to the surface creep observations is localized and near the surface and since creep events have been observed approximately simultaneously up to tens of kilometers apart [*C. Y. King et al.*, 1973], the question naturally arises as to how such failure patches can occur. It is possible that they are triggered by larger-scale deeper slip with a longer time scale.

If deeper slip is almost perfectly uniform, then little transient strain or tilt should be expected at observation points near the fault, although line length changes would be apparent in geodimeter data for lines spanning the fault at low angles [*Slater et al.*, 1976]. On the other hand, if deeper slip that eventually triggers near-surface creep events occurs over periods of days to weeks, then changes in strain should be evident also in continuous geodimeter data with these time scales. The approximate form and amplitude of the strains should follow those shown in the models in Figure 10, but with an expanded time scale. For example, a propagation velocity of 1 km/day would change the units on all the abscissas from hours to days.

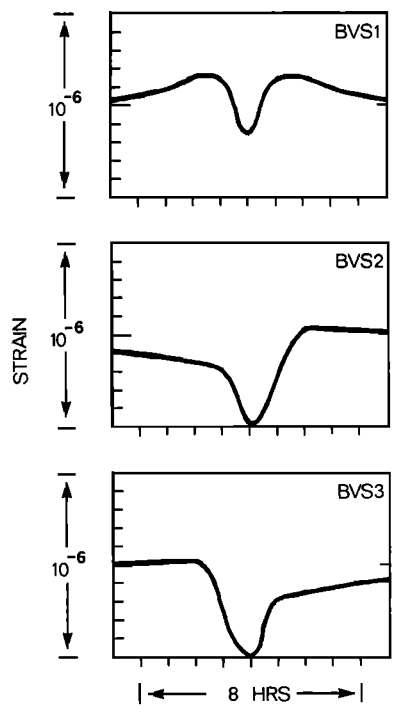

Fig. 9. Form and amplitude of strains expected at BVS1, BVS2, and BVS3 on the basis of *Frank*'s [1973] model for 5.0 mm of fault slip.

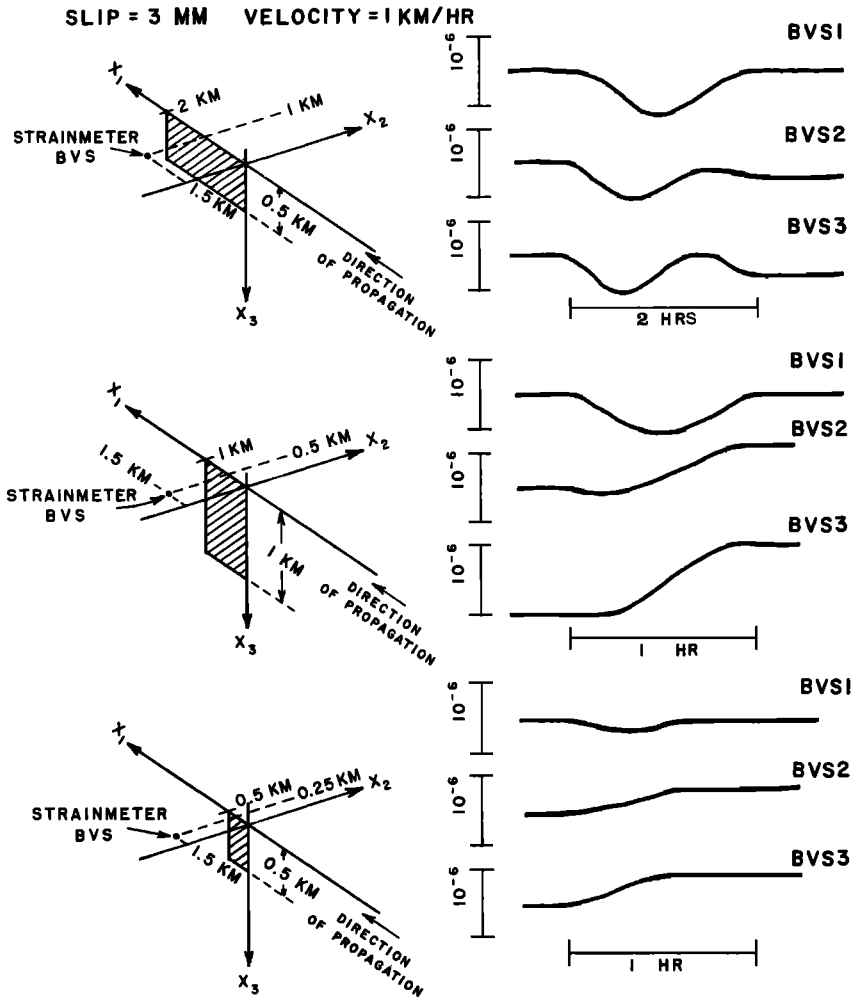

Fig. 10. Strains calculated at BVS1, BVS2, and BVS3 for a fault displacement of 3.0 mm as a function of geometry of the slipping section. Propagation velocity is chosen to be 1 km/h along the fault toward the northwest.

Unfortunately, noise, and therefore uncertainty of measurement, increases with period.

Changes in strain over periods of days to weeks, as illustrated in Figures 7 and 8, do occur at the times of creep events. Similar changes occur also at other times. It is possible that these changes reflect deeper slip that does not result in surface displacement. Since the shear strength of the fault probably increases with depth and since average fault displacement inferred from creep measurements agrees approximately with that inferred by geodetic measurements, slip at depth and surface slip must be intimately related.

There seems, at present, to be no unique way of determining whether any of the longer-term changes in Figures 7 and 8 are or are not creep related. Since slip models of the simplest kind cannot be fit to the data, the form is not consistent from event to event, and the signal amplitude does not increase with creep event amplitude, it seems most likely that these strain changes are not creep related.

A final question that should be asked concerns whether large dilatant strains, as discussed by *Frank* [1965], occur with creep events. Although localized dilatant strains may occur, large-scale dilatant strains at this distance from the fault are not evident either by inspection or by calculation of areal strain-time histories from the data. If transient dilatant strains do occur for these events, their amplitude cannot exceed 5×10^{-8} at this distance from the fault.

CONCLUSION

The average rate of fault displacement indicated by integrated surface creep measurements in the creeping section of the San Andreas fault presently amounts to more than 60% of the long-term rate of slip between the Pacific and North American plates [*Savage and Burford*, 1973; *Atwater and Molnar*, 1973]. The creep measurements are clearly of fundamental importance. In this attempt to understand the details of the episodic aspects of the creep observations, strains were measured to a sensitivity of 10^{-8} on three-component strainmeters at distances of 1.2–1.7 km from the San Andreas fault during 10 creep events. No clear observation of transient strain greater than 10^{-8} occurred coincident with or just preceding any of these events.

It would appear from simple models of these events that the transient strain fields have limited spatial extent and that the relevant parameter for fault mechanics discussions is average or smoothed creep. The episodic character probably results from the failure characteristics of near-surface materials (such as soils) and does not reflect the general fault behavior. Similar conclusions are also indicated in surface tilt measurements

around the fault during creep events [*Johnston et al.*, 1976; *McHugh and Johnston*, 1976; *Mortensen et al.*, 1977]. It is possible that this conclusion will be modified if the fault zone rigidity is substantially less than that of the surrounding material and strain and tilt fields attenuate more rapidly as a function of distance from the fault than might be expected on the basis of dislocation modeling in an elastic half space. Neither tidal response calculations nor seismic wave attenuation [*Healy and Peake*, 1975] indicates that this is the case.

Slip on the San Andreas fault apparently occurs more smoothly than was previously expected. In the longer-term data, however, there are no clear indications, at the 10^{-7} level, of deeper slip propagating at rates of a few kilometers per day that could load and generate episodic failure in the near-surface materials. In this case, it is more difficult to distinguish the transient strains from those due to tides or thermoelastic or meteorological effects. Detection of long-term transient strains of 10^{-8} generated by such deep slip would require removal of earth tidal strains and, perhaps, averaging of signals from several adjacent three-component strainmeters.

Acknowledgments. We thank R. O. Burford and Sandra Schulz for unpublished creep data.

REFERENCES

Atwater, T., and P. Molnar, Relative motion of the Pacific and North American plates deduced from sea-floor spreading in the Atlantic, Indian and South Pacific oceans, in *Proceedings of the Conference on Tectonic Problems of the San Andreas Fault System*, edited by R. L. Kovach and A. Nur, pp. 136–148, School of Earth Sciences, Stanford University, Stanford, Calif., 1973.

Beaumont, C., and J. Berger, Earthquake prediction: Modification of the earth tide tilts and strains by dilatancy, *Geophys. J. Roy. Astron. Soc., 39*, 111–121, 1974.

Bufe, C. G., and D. Tocher, Central San Andreas fault: Strain episodes, fault creep, and earthquakes, *Geology, 2*, 205–207, 1974.

Frank, F. C., On dilatancy in relation to seismic sources, *Rev. Geophys. Space Phys., 3*, 485–503, 1965.

Frank, F. C., Dislocation models for fault creep processes, *Phil. Trans. Roy. Soc. London, Ser. A, 274*, 351–354, 1973.

Gladwin, M. T., and J. Wolfe, Linearity of capacitance displacement transducers, *J. Sci. Instrum., 46*, 1099–1100, 1975.

Healy, J. H., and L. G. Peake, Seismic velocity structure along a section of the San Andreas fault near Bear Valley, California, *Bull. Seismol. Soc. Amer., 65*, 1177–1197, 1975.

Ida, T., Slow moving deformation pulses along tectonic faults, *Phys. Earth Planet. Interiors, 9*, 328–337, 1974.

Johnston, M. J. S., S. McHugh, and R. O. Burford, On simultaneous tilt and creep observations on the San Andreas fault, *Nature, 260*, 691–693, 1976.

King, C. Y., R. D. Nason, and D. Tocher, Kinematics of fault creep, *Phil. Trans. Roy. Soc. London, Ser. A, 274*, 355–360, 1973.

King, G. C. P., and R. G. Bilham, A geophysical wire strainmeter, *Bull. Seismol. Soc. Amer., 66*, 2039–2048, 1976.

King, G. C. P., R. G. Bilham, J. W. Campbell, D. P. McKenzie, and M. Naizi, Elastic strainfields due to fault creep events observed by invar wire strainmeters in Iran, *Nature, 253*, 420–423, 1975.

McHugh, S., Documentation of programs that compute (1) static tilts for a spatially variable slip distribution, (2) quasi-static tilts produced by a expanding dislocation loop with a spatially variable slip distribution, *Open File Rep. 76-578*, U.S. Geol. Surv., Washington, D. C., 1976.

McHugh, S., and M. J. S. Johnston, Some short-period nonseismic tilt perturbations and their relation to episodic slip on the San Andreas fault in central California, *J. Geophys. Res., 81*, 6341–6346, 1976.

McHugh, S., and M. J. S. Johnston, Surface shear stress, strain and shear displacement for screw dislocation in a vertical slab with shear modulus contrast, *Geophys. J. Roy. Astron. Soc., 49*, 715–722, 1977.

Mortensen, C. E., R. C. Lee, and R. O. Burford, Simultaneous tilt, strain, creep, and water level observations at the Cienega Winery south of Hollister, California, *Bull. Seismol. Soc. Amer., 67*, 641–650, 1977.

Nason, R. D., F. R. Philippsborn, and P. A. Yamashita, Catalog of creepmeter measurements in central California from 1968 to 1972. *Open File Rep. 74-31*, U.S. Geol. Surv., Washington, D. C., 1974.

Press, F., Displacements, strains, and tilts at teleseismic distances, *J. Geophys. Res., 70*, 2395–2412, 1965.

Savage, J. C., Theory of creep wave propagation, *J. Geophys. Res., 76*, 1954–1966, 1971.

Savage, J. C., and R. O. Burford, Geodetic determination of relative plate motion in California, *J. Geophys. Res., 78*, 832–845, 1973.

Slater, L. E., G. R. Hugget, and J. O. Langbein, Episodic fault slip in central California, *Eos Trans. AGU, 57*, 1012, 1976.

Stacey, F. D., J. M. W. Rynn, E. C. Little, and C. Croskell, Displacement and tilt transducers of 140 db range, *J. Sci. Instrum., 2*, 945–947, 1969.

Wesson, R., R. O. Burford, and W. L. Ellsworth, Relationship between seismicity, fault creep and crustal loading along the central San Andreas fault, in *Proceedings of the Conference on Tectonic Problems of the San Andreas Fault System*, edited by R. L. Kovach and A. Nur, pp. 303–321, School of Earth Sciences, Stanford University, Stanford, Calif., 1973.

Yamashita, P. A., and R. O. Burford, Catalogue of preliminary results from an 18-station creepmeter network along the San Andreas fault system in central California for the time interval June 1969–June 1973, open file report, U.S. Geol. Surv., Menlo Park, Calif., 1973.

(Received June 6, 1977;
revised August 19, 1977;
accepted August 23, 1977.)